Stem Cell Reports
Article

ISSCR

OPEN ACCESS

An *EWS-FLI1*-Induced Osteosarcoma Model Unveiled a Crucial Role of Impaired Osteogenic Differentiation on Osteosarcoma Development

Shingo Komura,[1,2] Katsunori Semi,[1,3] Fumiaki Itakura,[1] Hirofumi Shibata,[1] Takatoshi Ohno,[2] Akitsu Hotta,[1,3] Knut Woltjen,[1,4] Takuya Yamamoto,[1,3,5] Haruhiko Akiyama,[2] and Yasuhiro Yamada[1,3,*]

[1]Laboratory of Stem Cell Oncology, Department of Life Science Frontiers, Center for iPS Cell Research and Application (CiRA), Kyoto University, 53 Kawahara-cho, Shogoin, Sakyo-ku, Kyoto 606-8507, Japan
[2]Department of Orthopaedic Surgery, Gifu University Graduate School of Medicine, Gifu 501-1194, Japan
[3]Institute for Integrated Cell-Material Sciences (WPI-iCeMS), Kyoto University, Kyoto 606-8507, Japan
[4]Hakubi Center for Advanced Research, Kyoto University, Kyoto 606-8501, Japan
[5]AMED-CREST, AMED 1-7-1 Otemach, Chiyodaku, Tokyo 100-0004, Japan
*Correspondence: y-yamada@cira.kyoto-u.ac.jp
http://dx.doi.org/10.1016/j.stemcr.2016.02.009

SUMMARY

EWS-FLI1, a multi-functional fusion oncogene, is exclusively detected in Ewing sarcomas. However, previous studies reported that rare varieties of osteosarcomas also harbor *EWS-ETS* family fusion. Here, using the doxycycline-inducible *EWS-FLI1* system, we established an *EWS-FLI1*-dependent osteosarcoma model from murine bone marrow stromal cells. We revealed that the withdrawal of *EWS-FLI1* expression enhances the osteogenic differentiation of sarcoma cells, leading to mature bone formation. Taking advantage of induced pluripotent stem cell (iPSC) technology, we also show that sarcoma-derived iPSCs with cancer-related genetic abnormalities exhibited an impaired differentiation program of osteogenic lineage irrespective of the *EWS-FLI1* expression. Finally, we demonstrate that *EWS-FLI1* contributed to secondary sarcoma development from the sarcoma iPSCs after osteogenic differentiation. These findings demonstrate that modulating cellular differentiation is a fundamental principle of *EWS-FLI1*-induced osteosarcoma development. This in vitro cancer model using sarcoma iPSCs should provide a unique platform for dissecting relationships between the cancer genome and cellular differentiation.

INTRODUCTION

Cancer cells often exhibit similar properties to somatic stem/progenitor cells of the tissue of origin (Reya et al., 2001; Rossi and Weissman, 2006). Considering that progenitor cells at the developmental stage and somatic stem/progenitor cells in some adult tissues have the ability for self-renewal and/or active proliferation, it has been proposed that maintenance of the stem/progenitor cell state could be a driving force for tumor development (Reya et al., 2001). Osteosarcoma is a representative cancer that exhibits shared features with normal stem/progenitor cells (Luo et al., 2008; Thomas et al., 2004). The late markers of osteogenic differentiation are silenced while the early markers are modestly expressed in osteosarcomas (Luo et al., 2008; Thomas et al., 2004). Moreover, more aggressive phenotypes of osteosarcomas are correlated with features of early osteogenic progenitors (He et al., 2010; Luo et al., 2008), suggesting that defects in the osteogenic differentiation program may play a role in osteosarcoma development and progression. However, the causative aberrations that confer stem/progenitor cell properties on osteosarcoma cells are not fully understood.

EWS-FLI1, a widely recognized fusion oncogene for Ewing sarcomas, is generated by the chromosomal translocation of t(11;22) (q24;q12), which consists of the N-terminal transactivator domain of the *EWS* gene and the C-terminal ETS DNA binding domain of the *FLI1* gene. The resulting EWS-FLI1 fusion protein harbors multiple functions, acting as a transcriptional activator, transcriptional repressor, chromatin modulator, and splicing modulator (Kinsey et al., 2006; Riggi et al., 2014; Selvanathan et al., 2015; Smith et al., 2006). Despite the variety of oncogenic functions of *EWS-FLI1*, a number of previous studies implied that *EWS-FLI1* expression itself is not sufficient to induce Ewing sarcoma (Lin et al., 2008; Miyagawa et al., 2008; Riggi et al., 2008; Tanaka et al., 2015) and that other aberrations may be necessary. Indeed, genetic variants near *EGR2* and *TARDBP* are associated with susceptibility to Ewing sarcoma (Grunewald et al., 2015; Postel-Vinay et al., 2012). Moreover, additional genetic mutations, such as *TP53*, *CDKN2A*, and *STAG2*, have been identified in a subset of Ewing sarcomas (Crompton et al., 2014; Tirode et al., 2014). However, it remains unclear whether these mutations are additional driver mutations or passenger mutations and how they contribute to the sarcoma development.

The derivation of induced pluripotent stem cells (iPSCs) demonstrated that mammalian somatic cells can be reprogrammed into pluripotent stem cells (Takahashi and Yamanaka, 2006). It is noteworthy that the reprogramming process does not require any particular alterations to the

genetic information, which makes iPSC technology suitable to study the genotype-phenotype relationship in various diseases (Soldner et al., 2009; Yamashita et al., 2014). Considering that cancer is a genetic disease involving genetic mutations, single nucleotide variants, and structural abnormalities of the chromosome, iPSCs derived from cancer cells are expected to harbor shared genetic abnormalities with the parental cancer cells and therefore should be a powerful tool for dissecting the role of the cancer genome on the phenotype (Semi and Yamada, 2015).

Here, we established a murine *EWS-FLI1*-induced osteosarcoma model from adult bone marrow stromal cells using a doxycycline (Dox)-inducible-*EWS-FLI1* expression system. We revealed that *EWS-FLI1* expression inhibits the osteogenic differentiation of sarcoma cells in vitro and in vivo. Moreover, we found that iPSCs derived from the *EWS-FLI1*-induced osteosarcoma cells exhibit impaired osteogenic differentiation and give rise to sarcoma cells after osteogenic differentiation in vitro in conjunction with *EWS-FLI1* expression.

RESULTS

Establishment of *EWS-FLI1*-Inducible ESCs and Mice

First, we tried to establish an *EWS-FLI1*-inducible mouse model with locus targeting methods. We established two transgenic systems using embryonic stem cell (ESC) lines containing Dox-inducible *EWS-FLI1* alleles that were integrated at different loci by utilizing the KH2 system and *Rosa26* targeting vector (Figures 1A, S1A, and S1B) (Ohnishi et al., 2014; Yamada et al., 2013; Beard et al., 2006). In both ESC lines, reverse tetracycline-controlled transactivator (rtTA) is expressed from the *Rosa26* locus, and the Tet operator-*EWS-FLI1-ires-mCherry* construct is integrated into either the 3′UTR of the *Col1a1* locus (*Rosa-M2rtTA/Col1a1*::*tetO-EWS-FLI1*) or *Rosa26* locus (*Rosa-M2rtTA/Rosa*::*tetO-EWS-FLI1*). Both ESCs expressed mCherry fluorescence upon treatment with Dox in vitro (Figure 1B). The inducible *EWS-FLI1* expression in ESCs was also confirmed by qRT-PCR and western blotting (Figure 1C).

Next, we performed blastocyst injection of *EWS-FLI1*-inducible ESCs and obtained chimeric mice (Figure 1D and Table S1). Upon Dox treatment, *EWS-FLI1* was expressed in a wide variety of organs and tissues of the mice, including the bone marrow and the cortex of the bone where Ewing sarcomas often arise (Figures 1E, 1F, and S1C). Some mice (*Rosa-M2rtTA/Col1a1*::*tetO-EWS-FLI1*) died soon after *EWS-FLI1* induction, which was accompanied by dysplastic changes of intestinal cells due to impaired differentiation (8 of 14 mice, Figures 1G and S1D). However, despite the long-term induction of *EWS-FLI1* (up to 13 months), we did not observe any *EWS-FLI1*-dependent tumor formation in either system (Figure 1G).

Establishment of *EWS-FLI1*-Dependent Immortalized Cells with the Dox-Inducible *EWS-FLI1* Lentiviral System

Our results suggested that the induction of *EWS-FLI1* in adult mice is not sufficient for sarcoma development. Indeed, there is no report that shows the generation of *EWS-FLI1*-driven sarcomas by the targeted insertion of *EWS-FLI1* except for one study that reported the development of myeloid/erythroid leukemia (Torchia et al., 2007). However, previous studies have succeeded in modeling Ewing-like sarcomas in mice when combined with *Trp53* deletion or an integrating viral delivery system with the *EWS-FLI1* fusion gene, which is consistent with the hypothesis that additional genetic mutations may be required for *EWS-FLI1*-induced sarcoma development (Castillero-Trejo et al., 2005; Lin et al., 2008; Riggi et al., 2005; Tanaka et al., 2014).

Accordingly, we generated a lentiviral *EWS-FLI1* expression vector with the Dox-inducible expression system (Figure 2A). A *TetO-EWS-FLI1-ires-Neo* cassette was lentivirally transduced into bone marrow stromal cells from adult *Rosa26-M2rtTA/M2rtTA* mice (3–4 weeks of age). The transduced bone marrow cells were cultured with Dox and G418. The surviving cells were subsequently cultured for 2 months in culture medium containing Dox and G418. Although most cells with *EWS-FLI1*-inducible alleles did not survive, we nevertheless obtained three immortalized cell lines (EFN#2, EFN#12, and EFV#4; Figure 2B). The three lines expressed *EWS-FLI1* mRNA and protein in response to Dox (Figures 2C and 2D) and continuously proliferated under the Dox-containing culture condition (Figure 2B). Upon the withdrawal of Dox, the morphology of two cell lines (EFN#2 and EFN#12) gradually changed to a flat shape and proliferation was inhibited, whereas the third cell line (EFV#4) did not show any evidence of Dox dependency in terms of cellular kinetics (Figure S2A). These observations show that we obtained two *EWS-FLI1*-dependent immortalized cell lines from murine adult bone marrow stromal cells in vitro.

EWS-FLI1-Dependent Immortalized Cells Formed Osteosarcomas In Vivo

To confirm whether the *EWS-FLI1*-dependent immortalized cell lines have tumorigenic potential in vivo, we transplanted EFN#2 and EFN#12 into the subcutaneous layer of immunocompromised mice. At 10 weeks after the inoculation, the transplanted mice developed tumors from both cell lines when they were given Dox (16/16 for EFN#2, 2/4 for EFN#12; Figures 2E and 2F), whereas no tumor

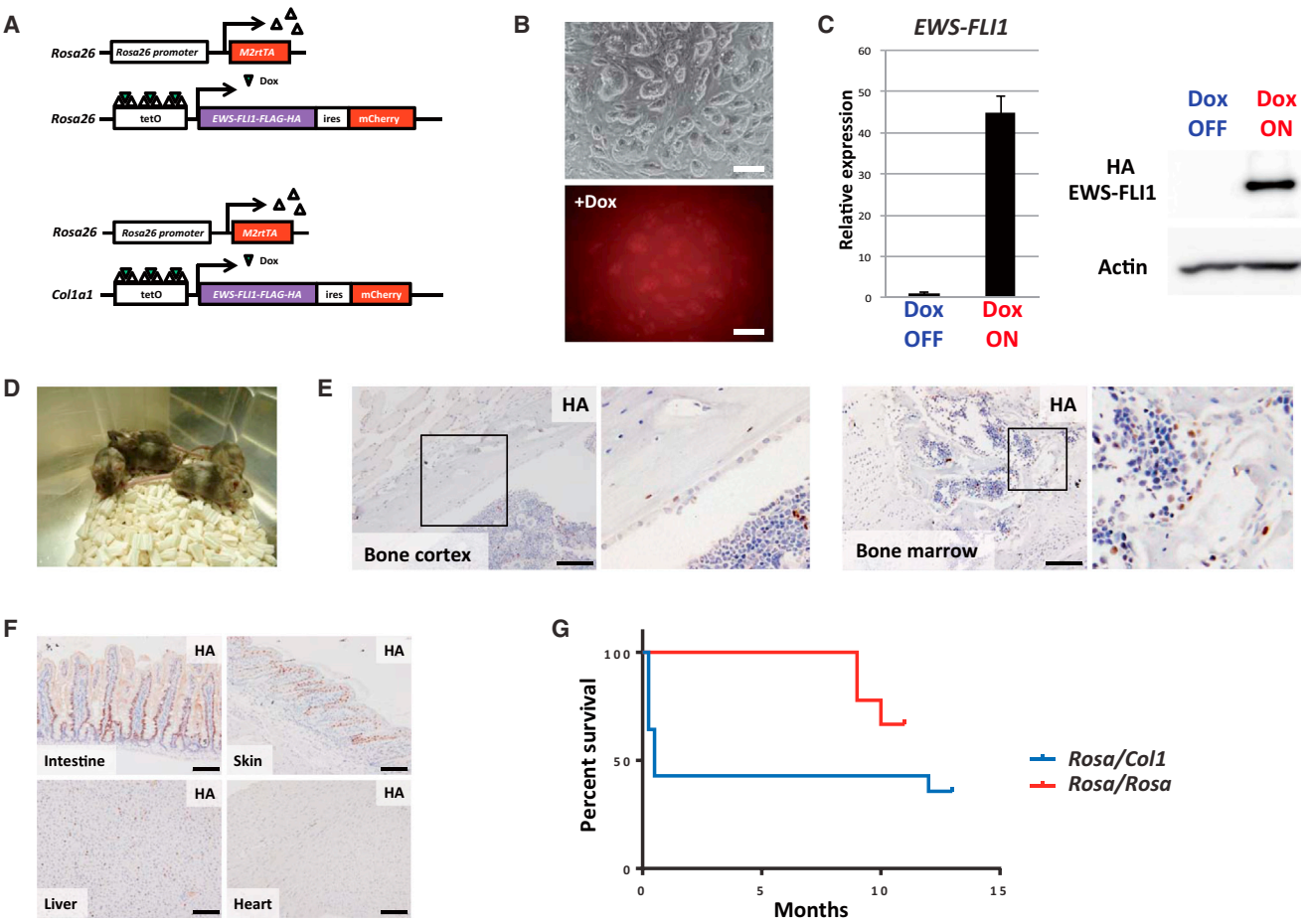

Figure 1. ESCs and Chimeric Mice with the Dox-Inducible *EWS-FLI1* Expression System

(A) Schematic illustrations of the Dox-inducible *EWS-FLI1* expression system. Two distinct ESC lines with Dox-inducible *EWS-FLI1* expression alleles targeted at different loci were established. Upward triangles (white), rtTA; downward triangles (green), Dox.

(B) *EWS-FLI1*-inducible ESCs (*Rosa-M2rtTA/Col1a1*::*tetO-EWS-FLI1-ires-mCherry*). The mCherry signal was detectable upon Dox exposure for 24 hr. Top, bright field; bottom, mCherry. Scale bars, 200 μm.

(C) *EWS-FLI1* mRNA and protein are detectable in ESCs upon Dox exposure for 24 hr. Data are presented as means ± SD (three technical replicates). The expression level of Dox OFF cells was set to 1. Similar results were obtained in both ESC lines.

(D) Chimeric mice were generated by injecting *EWS-FLI1*-inducible ESCs into blastocyst.

(E) Immunohistochemistry of various organs of chimeric mice treated with Dox for 2–7 days. Anti-HA antibody was used to detect EWS-FLI1 fusion protein. EWS-FLI1-positive cells are observed in the bone cortex and the bone marrow after treatment with Dox. Scale bars, 100 μm.

(F) EWS-FLI1-positive cells were observed in various organs after treatment with Dox. Scale bars, 100 μm.

(G) *EWS-FLI1* expression failed to generate sarcomas in chimeric mice derived from two ESCs. Some *Rosa-M2rtTA/Col1a1*::*tetO-EWS-FLI1* mice died in the early phase, presumably because of a gastrointestinal disorder (Figure S1D). Some mice died in the late phase because of *EWS-FLI1*-independent spontaneous cancer development such as lymphoma and lung cancer. *Rosa-M2rtTA/Col1a1*::*tetO-EWS-FLI1* mice, n = 14; *Rosa-M2rtTA/Rosa*::*tetO-EWS-FLI1* mice, n = 9.

formation was observed in mice without Dox administration (0/16 for EFN#2, 0/4 for EFN#12; Figures 2E and 2F). Histological analysis revealed that the tumors consisted of small round blue cells that resembled Ewing sarcomas. However, tumor cells often showed osteoid formation (Figures 2G and S2B) and thus were considered small-cell osteosarcoma, which is a rare subtype of osteosarcomas. In addition, immunohistochemistry showed that the tumor cells expressed EWS-FLI1 and were frequently positive for Ki67, a marker for proliferating cells (Figure S2B).

Establishment of *EWS-FLI1*-Dependent Osteosarcoma Cell Lines

To further investigate the properties of the *EWS-FLI1*-induced osteosarcomas in detail, we established *EWS-FLI1*-dependent osteosarcoma cell lines from subcutaneous

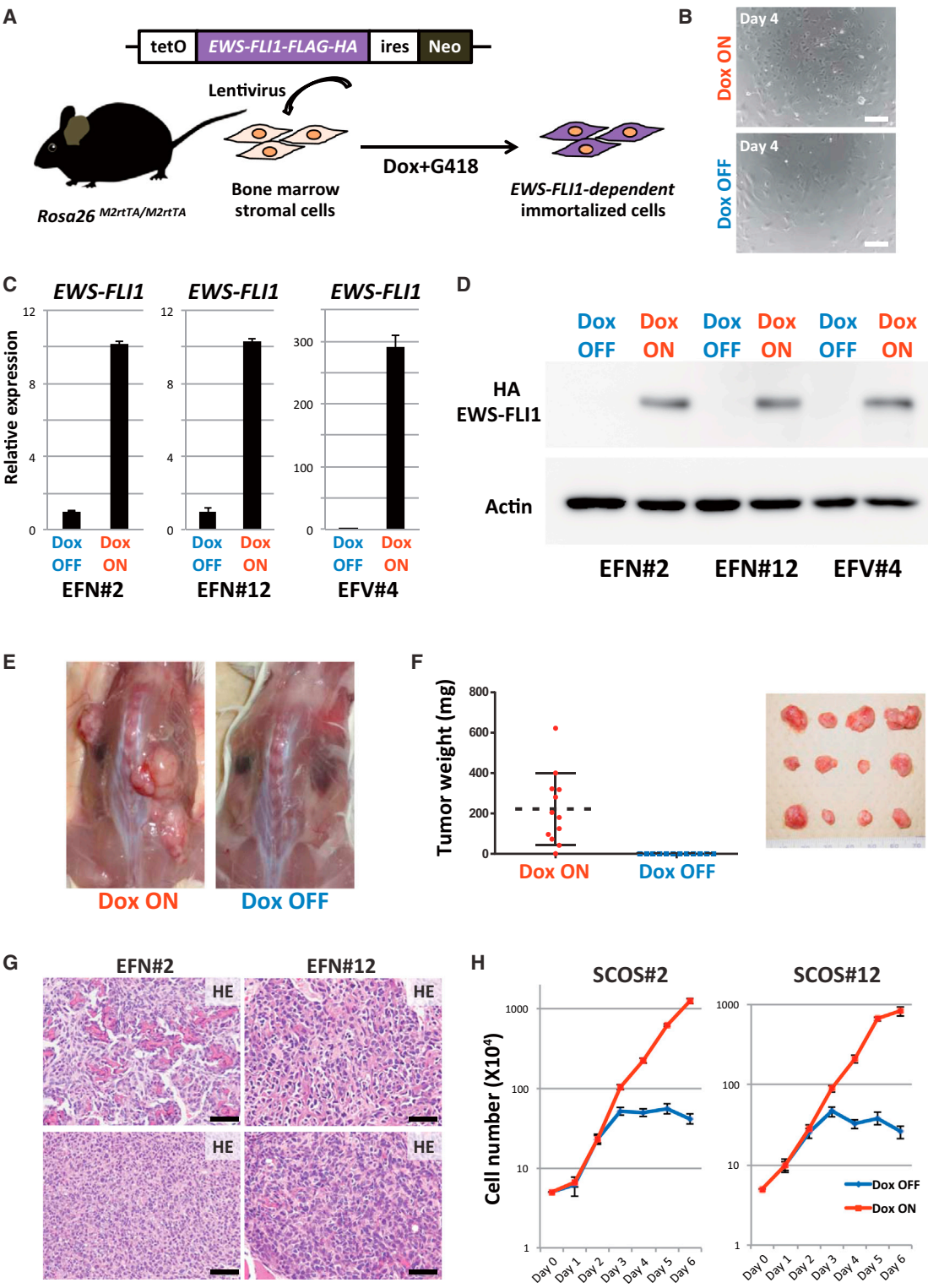

Figure 2. *EWS-FLI1*-Dependent Small-Cell Osteosarcoma Model by Utilizing the Lentiviral *EWS-FLI1* Expression System

(A) Schematic illustrations of the lentiviral *EWS-FLI1* expression system. Lentivirus was introduced into bone marrow stromal cells collected from *Rosa26-M2rtTA* mice. *EWS-FLI1*-expressing neomycin-resistant cells survived this protocol.

(legend continued on next page)

osteosarcomas in immunocompromised mice inoculated with EFN#2 and EFN#12 cells (SCOS#2 and SCOS#12, respectively). As observed in the primary *EWS-FLI1*-dependent immortalized cells, the established osteosarcoma cell lines expressed *EWS-FLI1* in a Dox concentration-dependent manner (Figure S2C) and actively proliferated in the presence of Dox (Figures 2H and S2D–S2F). After Dox withdrawal, SCOS#2 and SCOS#12 changed their morphology and stopped proliferating (Figure S2D). At the same time, we found increased expressions of p53 and p21, but no increase in β-gal (SAβgal) activity, which is associated with senescence (Figure S2G). Upon re-administration of Dox, the growth-arrested cells reacquired proliferative potential (Figure S2H). The reversible phenotype suggested that *EWS-FLI1* depletion results in cell-cycle arrest of the osteosarcoma cells.

Given that the genomic integration of lentivirus might play a role in osteosarcoma development, we also determined the virus integration site of SCOS#2. We identified a single integration at the intergenic region 13 kb downstream of *Cd14* (Figure S2I), a location unlikely to act as a genetic driver for sarcoma development.

To evaluate the similarity of the established *EWS-FLI1*-dependent sarcoma cell lines with human Ewing sarcomas and osteosarcomas, we compared global gene expression profiles of the SCOSs by microarray analysis. We first extracted genes that are specifically upregulated/downregulated in human Ewing sarcomas compared with human osteosarcomas and examined their expression in SCOS#2 and SCOS#12. We found that the gene expression patterns of SCOSs exhibit partial similarities with both human Ewing sarcomas and osteosarcomas (Figure S3A), suggesting that SCOSs have shared characteristics with both Ewing sarcomas and osteosarcomas.

Depletion of *EWS-FLI1* Expression Promoted Osteogenic Differentiation of Osteosarcoma Cells

To investigate the target of *EWS-FLI1*, we next compared gene expression profiles between *EWS-FLI1*-expressing and non-expressing sarcoma cells using SCOS#2 and SCOS#12. Intriguingly, in both cell lines, extracellular matrix and space-related genes, which often include bone and cartilage development-related genes, were significantly enriched in Dox OFF sarcoma cells (for 72 hr) compared with Dox ON *EWS-FLI1*-expressing sarcoma cells by GO enrichment analysis (Figures 3A, 3B, and S3B). Previous studies proposed that Ewing sarcoma could arise from mesenchymal stem cells (MSCs) (Riggi et al., 2008, 2014; Tirode et al., 2007). Long-term knockdown of *EWS-FLI1* with shRNA in Ewing sarcoma cells resulted in cellular differentiation to osteogenic, adipogenic, and chondrogenic lineage, consistent with an MSC origin of Ewing sarcoma (Tirode et al., 2007). Similarly, in the present study, the short-term depletion of *EWS-FLI1* in SCOS#2 and SCOS#12 resulted in the promotion of osteogenic differentiation with increased alkaline phosphatase activity (Figure 3C). Notably, after long-term depletion of *EWS-FLI1*, a subset of sarcoma cells slowly proliferated and exhibited heterogeneous morphology (Figure 3D). The *EWS-FLI1*-withdrawn sarcoma cells expressed higher levels of osteogenic differentiation marker genes, as well as chondrogenic and adipogenic genes (Figures 3E and S3C). Moreover, long-term culture without *EWS-FLI1* expression led to lipid production in a small subset of cells, as assessed by oil red O staining (Figure S3D).

SCOS#2 and SCOS#12 formed small-cell osteosarcomas in immunocompromised mice given Dox. These sarcoma cells had high proliferative activity based on Ki67 immunohistochemistry (Figure 3F). Consistent with in vitro findings that the growth of both SCOS#2 and SCOS#12 depends on *EWS-FLI1* expression, the subcutaneous tumors stopped or retarded their growth after the withdrawal of Dox in vivo (Figures 3F and 3G). Of particular note, histological analysis revealed that the Dox-withdrawn tumors consisted of osteoid and mature bone tissue with a small number of blue cells (Figure 3F). These results indicated that depletion of *EWS-FLI1* promoted osteogenic differentiation of

(B) The immortalized cells (EFN#2) grew rapidly in Dox-containing medium. Dox withdrawal resulted in growth retardation and morphological change in *EWS-FLI1*-expressing cells (4 days after the withdrawal). Scale bars, 200 μm.
(C) qRT-PCR results show *EWS-FLI1* mRNA expression in Dox-treated samples (24 hr). Data are presented as means ± SD (three technical replicates). The expression level of Dox OFF cells was set to 1.
(D) Western blotting using anti-HA antibody detected EWS-FLI1 protein in the presence of Dox (48 hr).
(E) *EWS-FLI1*-dependent immortalized cells (EFN#2) developed tumors in immunocompromised mice only in the presence of Dox (10 weeks after the transplantation).
(F) Tumor weight at 10 weeks after the transplantation of EFN#2 with/without Dox administration. Tumor development depended on Dox administration (n = 12, independent samples for each group). Error bars represent SD.
(G) Histology of *EWS-FLI1*-induced tumors in immunocompromised mice. Tumors are small-cell osteosarcomas, which consist of small blue round cells with various amounts of osteoid formation. The osteoid-rich region (upper) and small blue round cell-rich region (lower) are shown. Scale bars, 50 μm.
(H) Cell growth assay of the established *EWS-FLI1*-dependent sarcoma cell lines (SCOS#2 and SCOS#12). The growth of sarcoma cells depended on *EWS-FLI1* expression. Sarcoma cells without Dox exposure started to lose their growth at 3 days after Dox withdrawal. The means ± SD are shown in each group (two technical replicates per n; n = 3 biological replicates).

A

GO ACCESSION	GO Term	Corrected p-value
GO:0044421	extracellular region part	6.19E-18
GO:0005576	extracellular region	6.19E-18
GO:0031012	extracellular matrix	4.19E-10
GO:0005578	proteinaceous extracellular matrix	9.33E-09
GO:0005615	extracellular space	9.33E-09
GO:0005488	binding	1.37E-08
GO:0042127	regulation of cell proliferation	7.24E-08
GO:0008219	cell death	9.11E-07
GO:0016265	death	1.14E-06

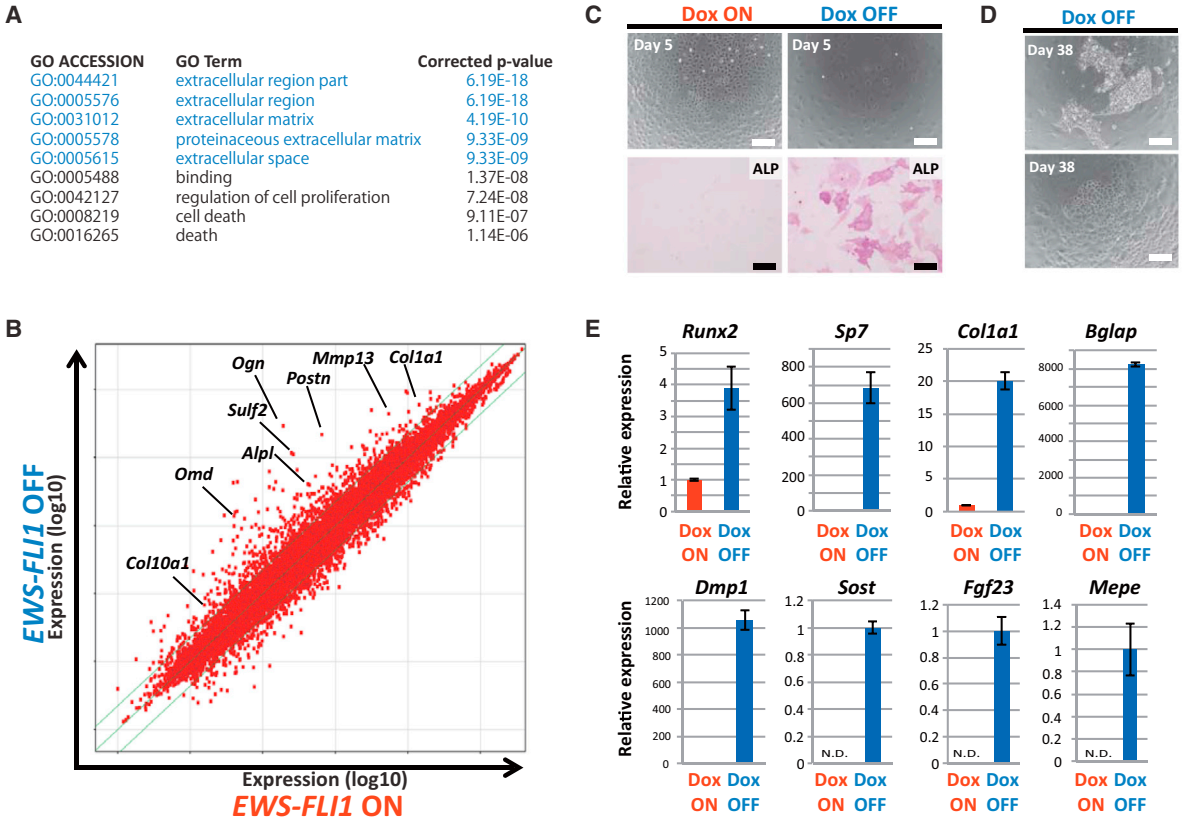

H

	Homer Known Motif	P-value	% of Targets	Best Match
1	ACTTTCGTTTCT	1E-35	2.42	T1ISRE
2	ATTTTCCATT	1E-22	20.17	NFATC1
3	ACGAGGAAGT	1E-22	12.76	ELF5(ETS)
4	ATTTCCTGTG	1E-18	13.58	EWS-ERG
5	GAGTTCCGGT	1E-18	13.58	Fli1
6	AACAGGAAAT	1E-17	8.58	EWS-FLI1

I

SK-N-MC (human Ewing sarcoma)

	De novo Motif	P-value	% of Targets	Best Match
1	ACGAAGGAAGGA	1E-1910	31.74	EWSR1-FLI1
2	AAGAAAGGAA	1E-600	35.04	EWSR1-FLI1
3	GAATGGAATGGA	1E-571	5.25	Zfp410
4	GATTTCCGGT	1E-435	18.29	ERG
5	TCTCGCGAGATC	1E-288	3.1	GFX

SCOS#2

	De novo Motif	P-value	% of Targets	Best Match
1	TAGTGGCTATCT	1E-182	12.60	Nkx2-6
2	ATTCTCGTCCTG	1E-171	18.18	AR-halfsite
3	TTGTGTCG	1E-171	16.97	Sox14
4	AAAAACAGGAAG	1E-157	12.02	Ets1
5	CTTGAAGAAA	1E-154	15.88	Tcfap2e

(legend on next page)

osteosarcoma cells in vivo. Together, our results highlight the role of *EWS-FLI1* expression on the suppression of terminal differentiation of osteosarcoma cells.

EWS-FLI1 Binds to the ETS Motif in *EWS-FLI1*-Induced Osteosarcoma Cells

To investigate how EWS-FLI1 suppresses the expression of osteogenic differentiation-related genes, we performed chromatin immunoprecipitation sequencing (ChIP-seq) analysis for hemagglutinin (HA)-tagged EWS-FLI1 in SCOS#2 cells using anti-HA antibody. The analysis identified 2,562 sites for EWS-FLI1 binding in *EWS-FLI1*-expressing SCOS#2. A motif analysis with HOMER (hypergeometric optimization of motif enrichment) revealed that these binding sites often contain the ETS binding motif (Figure 3H), suggesting that EWS-FLI1 binds to the genome through the C-terminal ETS binding domain of FLI1. Previous studies demonstrated that EWS-FLI1 binds DNA preferentially at GGAA repeats to activate transcription. Indeed, we confirmed that the GGAA repeat is the most representative motif of EWS-FLI1 binding in SK-N-MC, a human Ewing sarcoma cell line (Figure 3I) (Riggi et al., 2014). Notably, the GGAA repeat was not enriched in SCOS#2 according to de novo motif analysis for EWS-FLI1 binding (Figure 3I).

One target of EWS-FLI1 in human Ewing sarcoma, *Nr0b1*, has 15 GGAA repeats 50 kb upstream from its transcription start site (TSS) in mouse. ChIP-seq data revealed that EWS-FLI1 does not bind to these GGAA repeats in SCOS#2, which is consistent with the fact that *Nr0b1* expression is not affected by EWS-FLI1 expression in SCOS#2 (data not shown). We found similar GGAA repeats upstream and downstream of *Nkx2-2*, *Ccnd1*, and *Dkk2*, which are also known targets of EWS-FLI1 binding in human Ewing sarcomas. However, there was no clear enrichment of EWS-FLI1 binding in SCOS#2. Ultimately, we found that only four of 2,562 EWS-FLI1 binding sites in SCOS#2 contained more than ten GGAA repeats, highlighting the difference in EWS-FLI1 binding between human Ewing sarcomas and our *EWS-FLI1*-induced osteosarcoma cells.

To further assess whether EWS-FLI1 binding affects the expression of adjacent genes, we first identified 126 genes that possess EWS-FLI1 binding sites close to their TSS (±5 kb) and compared the expression between Dox (*EWS-FLI1*) ON and Dox OFF cells. No obvious difference in the expression levels of these genes was detected (Figure S4A). Similarly, EWS-FLI1 binding was not enriched near the TSSs of the genes upregulated or downregulated by Dox exposure (517 and 588 genes, respectively; cutoff point at fold change >1.5; Figure S4B). In contrast, the genome-wide analysis of EWS-FLI1 binding revealed that EWS-FLI1 was preferentially recruited to the distal intergenic region (72.5% of total binding sites) (Figures S4C and S4D). Our results indicate that EWS-FLI1 binds to the genome via the ETS motif, but EWS-FLI1 binding at the proximal regulatory region does not have a substantial impact on altered gene expressions in *EWS-FLI1*-induced osteosarcoma cells.

Establishment of iPSCs from *EWS-FLI1*-Induced Osteosarcoma Cells

The derivation of iPSCs does not require specific changes in the genomic sequence, making this technology applicable for the evaluation of genetic context effects on cell types and differentiation statuses. Given that additional genetic aberrations may be required for *EWS-FLI1*-induced sarcoma development, the establishment of iPSCs from *EWS-FLI1*-induced sarcoma cells should provide a unique

Figure 3. Inhibition of Osteogenic Differentiation by *EWS-FLI1* in Small-Cell Osteosarcoma Cells

(A) Gene ontology enrichment analysis showed that the extracellular region and matrix-related genes are upregulated 72 hr after Dox withdrawal in SCOS#2 cells. The upregulated genes were selected by cutoff point at hold change >1.5 and $p < 1.0 \times 10^{-4}$. The top five enriched clusters are highlighted.

(B) Scatterplot analysis revealed that a number of osteogenesis and chondrogenesis-related genes were upregulated 72 hr after Dox withdrawal in SCOS#2 cells.

(C) At 5 days after Dox withdrawal, sarcoma cells exhibited alkaline phosphatase activity. Scale bars, 50 μm (upper) and 200 μm (lower).

(D) At 38 days after Dox withdrawal, slow-growing heterogeneous cells were observed. Scale bars, 200 μm.

(E) At 38 days after Dox withdrawal, cells showed higher expression of osteogenic differentiation-related genes. mRNA expression levels were measured by qRT-PCR. Data are presented as means ± SD (three technical replicates). The expression level of Dox ON cells was set to 1. *Sost*, *Fgf23*, and *Mepe* were undetectable in Dox ON samples by qRT-PCR, therefore, the expression level of Dox OFF cells was set to 1 instead.

(F) H&E and alizarin red staining demonstrated that Dox withdrawal leads to a significant reduction of the small blue cell population and an increase of mature bone formation. Ki67 immunohistochemistry shows the active proliferation of sarcoma cells in Dox ON condition. Scale bars, 200 μm (upper) and 50 μm (lower).

(G) In vivo tumor formation assay using sarcoma cell line SCOS#2 (n = 7, independent tumor). Dox treatment was withdrawn at 3 weeks, and mice were sacrificed at 7 weeks.

(H) The ETS motif was enriched in EWS-FLI1 binding sites according to motif analysis with HOMER of SCOS#2.

(I) De novo motif analysis identified the GGAA repeat as the most frequent motif in SK-N-MC. This repeat was not found in SCOS#2.

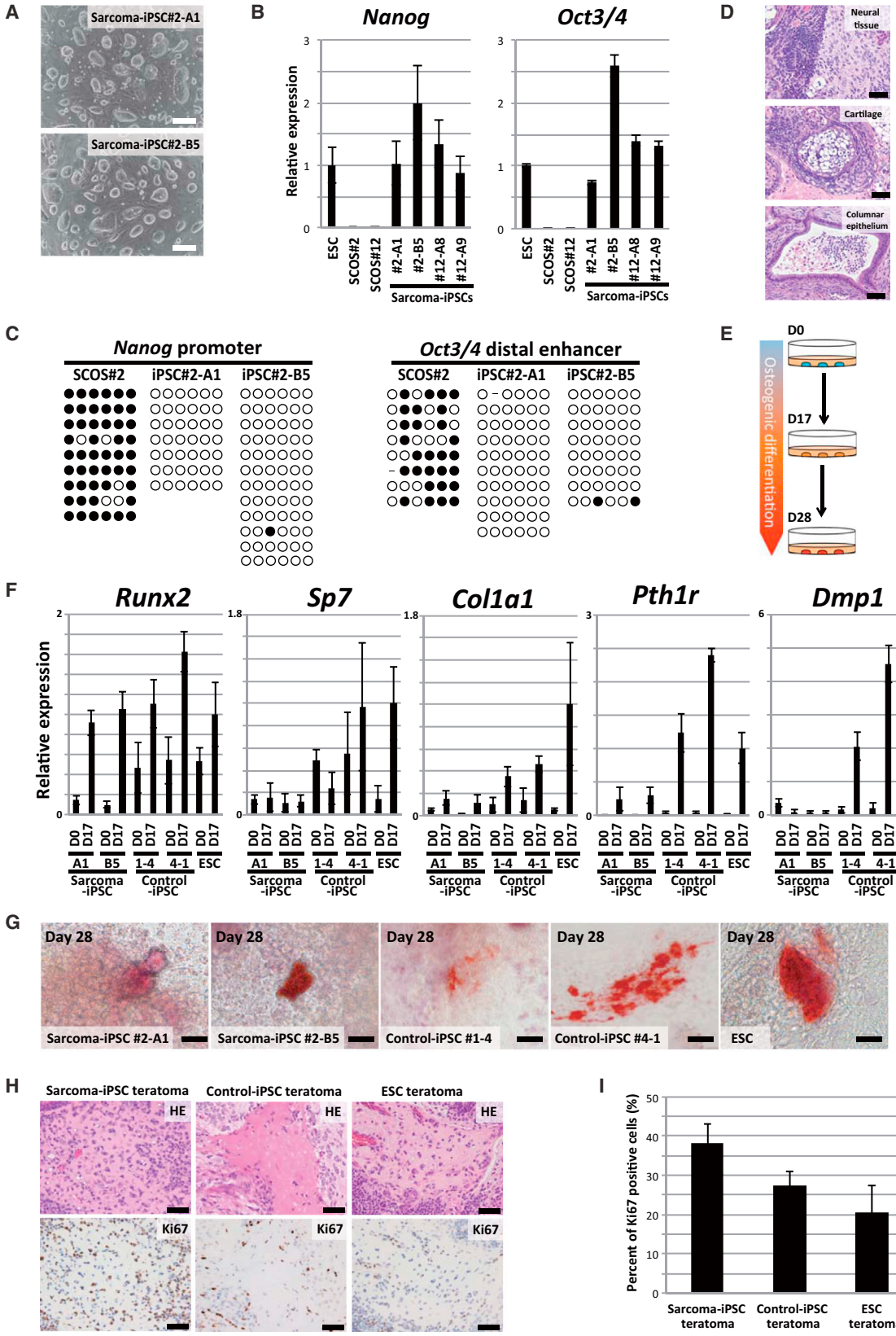

(legend on next page)

tool to study the impact of genetic abnormalities beyond *EWS-FLI1* expression on sarcoma development. We therefore tried to establish iPSCs from SCOS#2 and SCOS#12. After single-cell cloning of sarcoma cells, we introduced *OCT3/4, SOX2, KLF4*, and *c-MYC* into the sarcoma cells and obtained iPSC-like colonies under the absence of *EWS-FLI1* expression (efficiency of colony formation was 0.0009%; Figures 4A and S5A). These iPSC-like cells expressed pluripotency-related genes, such as *Nanog* and *Oct3/4*, at comparative levels with ESCs (Figure 4B). Similarly, the global gene expression patterns of iPSC-like cells were similar to those in normal ESCs and control iPSCs (Figure S5B).

The sarcoma-derived iPSC-like cells exhibited demethylation of both *Nanog* promoter and *Oct3/4* distal enhancer (Figure 4C), implying that these cells underwent epigenetic reorganization to acquire pluripotency. The silencing of the four exogenous factors, which occurs in the late stage of cellular reprogramming, was observed in some iPSC-like clones (Figure S5C), suggesting that these cells were fully reprogrammed. Then, we performed array comparative genomic hybridization (array CGH) and found that the single-cell-derived sarcoma cells had extensive chromosomal abnormalities (Figure S5D). Notably, sarcoma-derived iPSC-like cells harbored some identical chromosomal aberrations (Figure S5D). Furthermore, exome analysis revealed hundreds of identical missense mutations between SCOS#2 and sarcoma-derived iPSC-like cells (Figure S5E and Table S2), affirming that these iPSC-like clones were derived from the parental sarcoma cell. A subset of the mutated genes was also mutated in human Ewing sarcomas and osteosarcomas by the COSMIC database (http://cancer.sanger.ac.uk/cosmic) (Table S3). These sarcoma-derived iPSC-like cells lacked the ability to contribute to adult chimeric mice by blastocyst injection (data not shown), presumably because of the extensive genetic abnormalities observed in the CGH analysis and exome analysis. However, sarcoma-derived iPSC-like cells formed teratomas consisting of cells differentiating into three different germ layers when they were inoculated into the subcutaneous tissue of immunocompromised mice (Figure 4D), indicating that they have pluripotency. These results affirm that we succeeded in generating iPSCs from *EWS-FLI1*-induced osteosarcoma cells.

Sarcoma iPSCs Exhibit Impaired Osteogenic Differentiation Irrespective of *EWS-FLI1* Expression

The enhanced osteogenic differentiation of sarcoma cells upon the depletion of *EWS-FLI1* raised the possibility that *EWS-FLI1*-dependent osteosarcomas arise from osteogenic cells. Accordingly, we tried to induce osteogenic cells, a putative cell of origin of the sarcomas, from pluripotent stem cells in vitro in the absence of *EWS-FLI1* expression (Figure 4E) (Kim et al., 2010). In control ESCs and control iPSCs established from the fibroblasts of *EWS-FLI1*-inducible chimeric mice (*Rosa-M2rtTA/Rosa:tetO-EWS-FLI1*), osteogenic differentiation stimuli induced osteogenic differentiation-related genes, such as *Runx2, Sp7, Col1a1, Pth1r*, and *Dmp1* (day 17) (Figure 4F). Although the stimuli also induced the expression of *Runx2*, a key transcription factor for osteogenic

Figure 4. Establishment of Sarcoma-Derived iPSCs and Differentiation of Sarcoma iPSCs into Osteogenic Cells

(A) iPSCs-like cells were established from sarcoma cells by introducing reprogramming transcription factors. Scale bars, 200 μm.

(B) qRT-PCR revealed that the expression levels of pluripotency-related genes in sarcoma-derived iPSC-like cells were equivalent to those of ESCs. Data are presented as means ± SD (three technical replicates). The expression level of ESCs was set to 1.

(C) Bisulfite sequencing analyses revealed that the *Nanog* promoter and the *Oct3/4* distal enhancer region are demethylated in sarcoma-derived iPSC-like cells. White and black circles indicate non-methylated and methylated cytosine at CpG sites, respectively.

(D) Sarcoma iPSCs gave rise to teratomas consisting of ectodermal, mesodermal, and endodermal tissue in the subcutaneous tissue of immunocompromised mice. Scale bars, 50 μm.

(E) Schematic illustrations of in vitro osteogenic differentiation.

(F) qRT-PCR analysis of osteogenic differentiation-related genes. Wild-type ESCs (V6.5), *EWS-FLI1*-inducible ESCs (*Rosa-M2rtTA/Rosa::tetO-EWS-FLI1*), and two independent fibroblast-derived iPSCs with *Rosa-M2rtTA/Rosa::tetO-EWS-FLI1* alleles were used as controls in the osteogenic differentiation experiments. Sarcoma-derived iPSCs and control ESCs/iPSCs on day 0 and day 17 during osteogenic differentiation were examined for the expression of osteogenic differentiation-related genes. The mean ± SD is shown (three technical replicates per n; n = 3 biological replicates). The mean expression level of ESCs on day 17 was set to 1.

(G) Alizarin red staining revealed extracellular calcium deposits stained in blight reddish orange (day 28 after the induction of osteogenic differentiation). Scale bars, 20 μm.

(H) Histological analysis of an osteogenic region with osteoid production in teratomas. Ki67 immunohistochemistry revealed that osteoid-producing cells derived from sarcoma iPSCs have higher proliferative activities than those derived from control ESCs/iPSCs. Scale bars, 50 μm.

(I) Ki67 positive ratio of osteogenic regions in teratomas derived from sarcoma iPSCs or control ESCs/iPSCs. The mean ± SD of six independent osteogenic regions in two independent sarcoma iPSCs teratomas, five independent osteogenic regions in the control iPSC teratomas, and nine independent osteogenic regions in two independent ESC teratomas are shown. The ANOVA test was used for the statistical analysis. Sarcoma iPSCs vs control iPSCs, $p < 0.05$; sarcoma iPSCs vs control ESCs, $p < 0.01$; control ESCs vs control iPSCs, $p > 0.05$.

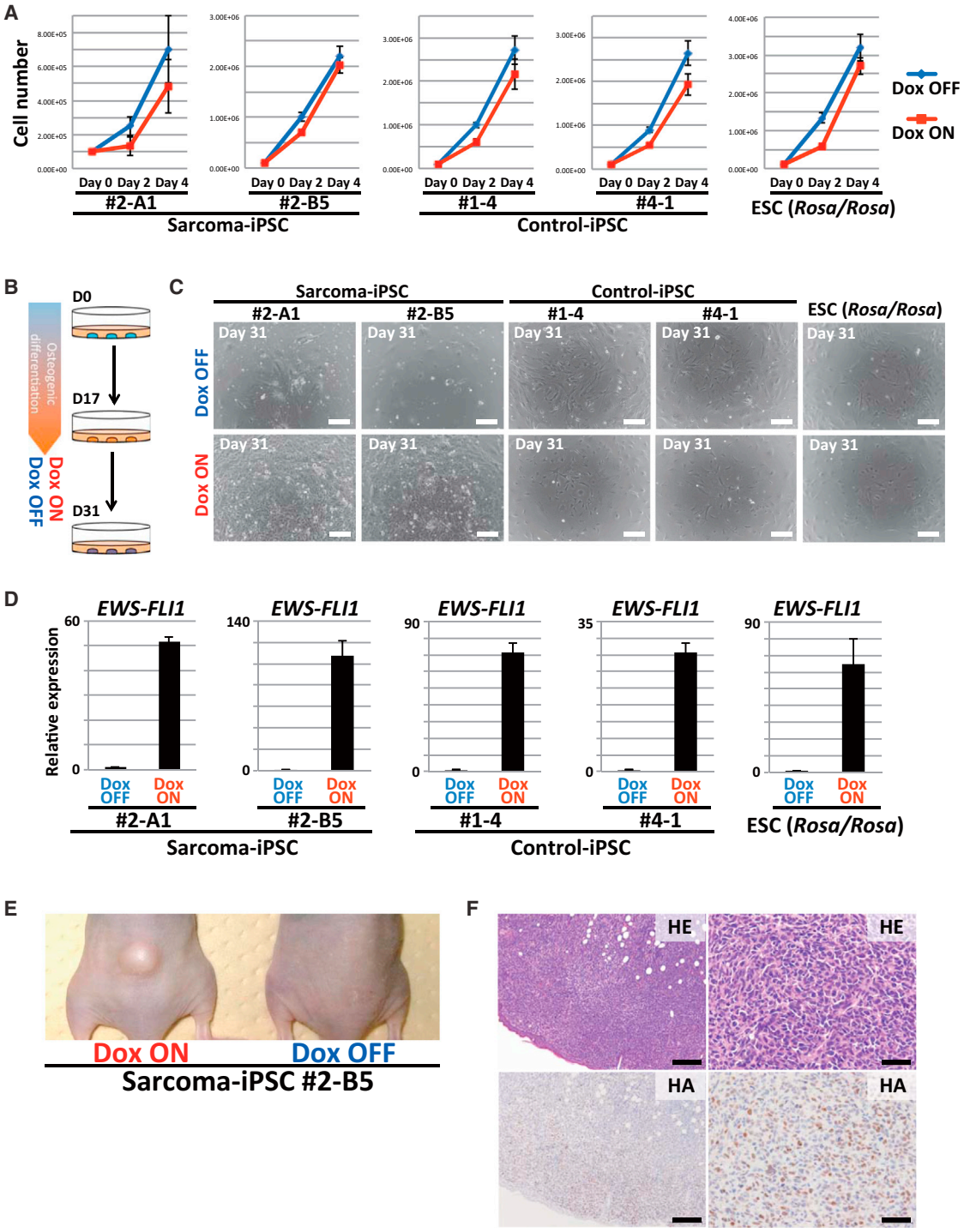

Figure 5. *EWS-FLI1* Induces Sarcomas from Induced Osteogenic Cells in Concert with Genetic Aberrations

(A) *EWS-FLI1* expression does not promote the growth of undifferentiated pluripotent stem cells. The means ± SD are shown in each group (two technical replicates per n; n = 3 biological replicates).

(B) Schematic illustration of in vitro osteogenic differentiation and *EWS-FLI1* induction. The induced osteogenic cells (17 days after the induction of osteogenic differentiation) were subsequently treated with/without Dox for 2 weeks.

(C) The sarcoma iPSC-derived osteogenic cells acquired robust proliferation with Dox treatment, whereas control ESCs/iPSCs (*Rosa-M2rtTA/Rosa*::*tetO-EWS-FLI1*)-derived osteogenic cells did not. Scale bars, 200 μm.

(legend continued on next page)

differentiation, in sarcoma-derived iPSCs, the induction of osteogenic genes downstream of *Runx2* was impaired even in the absence of *EWS-FLI1* expression (day 17) (Figure 4F). Upon the prolonged induction of osteogenic differentiation (day 28), a mineralized region, as assessed by alizarin red staining, was detected in all samples (Figure 4G). However, the mineralized area was larger in control ESCs/iPSCs than in sarcoma-derived iPSCs (Figure 4G). We also employed the in vivo differentiation method of sarcoma iPSCs to generate teratomas in immunocompromised mice. Both the sarcoma iPSCs and the control ESCs/iPSCs formed teratomas, which contained an osteogenic region in the absence of *EWS-FLI1* expression (Figure 4H). The Ki67-positive ratio of sarcoma iPSC-derived osteogenic cells was significantly higher than that of control ESC/iPSC-derived osteogenic cells ($p < 0.05$ and $p < 0.01$, respectively) (Figure 4I). Collectively, sarcoma-derived iPSCs exhibit impaired osteogenic differentiation irrespective of *EWS-FLI1* expression, suggesting that genetic and epigenetic alterations besides *EWS-FLI1* fusion also inhibit osteogenic differentiation and maintain the proliferating progenitor state.

EWS-FLI1 Expression Induced Rapid Sarcoma Development from Sarcoma iPSC-Derived Osteogenic Cells

Finally, we tried to analyze the cooperative action between *EWS-FLI1* expression and the impaired differentiation associated with genetic aberrations on sarcoma development. *EWS-FLI1* expression in both sarcoma iPSCs and control ESCs/iPSCs (*Rosa-M2rtTA/Rosa*::*tetO-EWS-FLI1*) has no promoting effect on cell growth under undifferentiated culture conditions (Figure 5A). Next, we induced osteogenic differentiation of sarcoma iPSCs and control cells in vitro and then *EWS-FLI1* expression (Figure 5B). At day 17 of the osteogenic differentiation protocol, osteogenic precursor cells derived from sarcoma iPSCs and control cells were treated with Dox (Figure 5B). Of note, only the sarcoma-derived osteogenic cells showed robust proliferation in vitro in response to Dox at day 31 (Figures 5C and 5D). Xenograft of these cells resulted in tumor development only in mice given Dox (Figure 5E). Histological analysis revealed that these xenograft tumors were sarcomas that consisted of small round blue cells (Figure 5F). The secondary sarcoma harbored shared genetic mutations with SCOS (Figure S5E and Table S2). Osteogenic cells derived from control ESCs/iPSCs did not exhibit obvious *EWS-FLI1*-dependent growth in vivo (data not shown), affirming that sarcoma development requires additional aberrations. Interestingly, these tumors often contained a carcinoma component, therefore they were regarded as carcinosarcomas (Figure S5F). Presumably, this component reflected the contamination of heterogeneous cell types after in vitro osteogenic differentiation of the sarcoma iPSCs. Together, these results suggest that the impaired differentiation potential associated with the sarcoma genome contributes to a rapid malignant transformation of osteogenic cells upon *EWS-FLI1* expression.

DISCUSSION

Although the exact cell of origin of Ewing sarcoma remains to be determined, it is suggested that Ewing sarcomas may arise from MSCs, which reside in the bone marrow (Riggi et al., 2008; Tirode et al., 2007). In the present study, we introduced the *EWS-FLI1* fusion gene to bone marrow stromal cells to establish an Ewing sarcoma mouse model (Castillero-Trejo et al., 2005; Riggi et al., 2005). We successfully generated *EWS-FLI1*-induced sarcomas that depended on *EWS-FLI1* expression in terms of in vitro proliferation and in vivo tumor development. However, the developed tumors were small-cell osteosarcomas composed of small round blue cells with osteoid formation. Small-cell osteosarcoma is a rare subtype of osteosarcomas, accounting for 1%–1.5% of all osteosarcomas (Nakajima et al., 1997). Notably, small-cell osteosarcoma exhibits shared properties with Ewing sarcoma (Righi et al., 2015). Moreover, *EWSR1* rearrangement, which includes *EWS-FLI1*, has been identified in a subset of small-cell osteosarcomas (Dragoescu et al., 2013; Hill et al., 2002; Noguera et al., 1990; Oshima et al., 2004). The results of the present study demonstrate that the *EWS-FLI1* fusion gene could function as a driver oncogene in a particular type of osteosarcoma and suggest that our model could be a rodent model for *EWS-FLI1*-dependent osteosarcomas.

The inhibition of differentiation has been considered to play a role in many types of tumor development through maintenance of the proliferating progenitor cell state. Previous studies demonstrated that the knockdown of *EWS-FLI1* in Ewing sarcoma cell lines results in osteogenic, adipogenic and chondrogenic differentiation (Tirode et al., 2007). Similarly, in the present study, we found that

(D) *EWS-FLI1* expression in the induced osteogenic cells was detectable by Dox exposure in qRT-PCR analyses. Data are presented as means ± SD (three technical replicates). The mean expression level of Dox OFF was set to 1.
(E) Osteogenic cells induced with *EWS-FLI1* developed tumors in immunocompromised mice only in the presence of Dox (after 3–7 weeks of treatment).
(F) Histologically, developed tumors were sarcomas consisting of small round blue cells that resembled small-cell osteosarcomas. HA immunohistochemistry revealed that sarcoma cells express EWS-FLI1. Scale bars, 200 μm (left) and 50 μm (right).

EWS-FLI1-induced osteosarcomas exhibit robust osteogenic differentiation after the withdrawal of *EWS-FLI1* expression, indicating that *EWS-FLI1* expression inhibits osteogenic differentiation. Molecular mechanisms by which *EWS-FLI1* expression blocks osteogenic differentiation have been proposed in previous studies. It was reported that EWS-FLI1 inhibits osteogenic differentiation in murine multipotent mesenchymal cells by binding to Runx2, an osteogenic transcription factor, and inhibiting its function (Li et al., 2010). Similarly, EWSR1 was shown to interact with SOX9, which is involved in chondrogenic differentiation in zebrafish (Merkes et al., 2015). However, we failed to detect a physical interaction between EWS-FLI1 and Runx2 or Sox9 in our osteosarcoma cells by immunoprecipitation (data not shown), suggesting that another mechanism may exist for the defective differentiation. Notably, Riggi et al. (2014) demonstrated that EWS-FLI1 expression causes the displacement of endogenous ETS transcription factors and p300 at the canonical ETS motifs in Ewing sarcoma cells. We found that EWS-FLI1 binds to the genome through the ETS motif in *EWS-FLI1*-dependent osteosarcoma cells. Given that the ETS family of transcription factors plays an important role in osteogenic differentiation as well as adipogenic and chondrogenic differentiation (Birsoy et al., 2011; Iwamoto et al., 2007; Raouf and Seth, 2000), the aberrantly occupied ETS motifs by EWS-FLI1 might inhibit ETS family-mediated differentiation, resulting in maintenance of the proliferating progenitor state.

The majority of Ewing sarcomas arise in adolescence. Considering the young age at onset, it is suggested that Ewing sarcoma harbors few genetic abnormalities besides the *EWS-FLI1* fusion gene. Indeed, recent genome-wide sequencing analyses revealed a paucity of somatic abnormalities (Crompton et al., 2014; Tirode et al., 2014). However, consistent with a number of previous studies, we failed to induce sarcomas by the sole expression of *EWS-FLI1* in a variety of cell types in vivo, providing additional evidence that *EWS-FLI1* expression is not sufficient for sarcoma development. Thus, we established iPSCs from *EWS-FLI1*-induced osteosarcoma cells, thereby harboring the same genetic abnormalities as the parental osteosarcoma cells. Interestingly, upon the induction of osteogenic differentiation, *EWS-FLI1* expression turned sarcoma iPSC-derived osteogenic cells into sarcoma cells, whereas the expression was not sufficient for the transformation of those from control ESCs/iPSCs.

It is noteworthy that sarcoma iPSCs showed an impairment of terminal osteogenic differentiation ability irrespective of *EWS-FLI1* expression. Notably, we found that osteogenic lineage cells derived from sarcoma iPSCs exhibit higher proliferating activity compared with cells derived from control ESCs/iPSCs. Taken together, it is conceivable that the additive effect by both *EWS-FLI1* expression and the defective differentiation properties of sarcoma iPSCs promotes sarcoma development by suppressing terminal differentiation and maintaining the proliferating progenitor state.

The causative aberration of the impaired differentiation properties of sarcoma iPSCs remains unclear. Recently, Lee et al. (2015) established iPSCs from patients with Li-Fraumeni syndrome and demonstrated that mutant p53 causes defective osteoblastic differentiation. However, we failed to detect the *Trp53* mutation in our sarcoma-derived iPSCs (Table S2), implying an alternative mechanism impairs osteogenic differentiation. Intriguingly, we observed that sarcoma iPSC teratomas sometimes exhibited impaired terminal differentiation of other lineages, which is also consistent with the fact that they lack the potential to make chimeric mice (Figure S5G). It is likely that a summation of extensive genetic abnormalities and epigenetic alterations is associated with the impaired differentiation of sarcoma iPSCs into multiple lineages. Further analysis is needed to determine the aberrations required for the sarcoma development associated with *EWS-FLI1* expression.

The fact that the in vitro induction of osteogenic differentiation leads to sarcoma development from sarcoma iPSCs in concert with *EWS-FLI1* expression indicates that these sarcomas arise from osteogenic progenitor cells. However, it is important to note that the withdrawal of *EWS-FLI1* in osteosarcoma cells resulted in increased expression of multiple genes involved in chondrogenic and adipogenic differentiation in addition to osteogenic differentiation-related genes. Together with previous findings on Ewing sarcoma, multipotent progenitors that have partial commitment to the osteogenic lineage in the bone marrow could be a cell of origin for *EWS-FLI1*-induced osteosarcomas. This notion is also supported by the fact that a subset of small-cell osteosarcomas exhibits both chondrogenic and osteogenic differentiation (Dragoescu et al., 2013; Nakajima et al., 1997).

In summary, we established an *EWS-FLI1*-dependent small-cell osteosarcoma model by introducing *EWS-FLI1* in mouse bone marrow stromal cells. We revealed that the impaired differentiation associated with both *EWS-FLI1* expression and sarcoma-associated genetic abnormalities plays a critical role in the development and maintenance of *EWS-FLI1*-induced osteosarcomas. We propose that targeting impaired terminal differentiation could be a possible therapeutic strategy for *EWS-FLI1*-induced sarcomas.

EXPERIMENTAL PROCEDURES

In Vivo Experiment

Rosa-M2rtTA/Rosa:tetO-EWS-FLI1 and *Rosa-M2rtTA/Col1a1::tetO-EWS-FLI1* chimeric mice were generated with KH2 (Beard et al., 2006). *Rosa-M2rtTA/Rosa::tetO-EWS-FLI1* mice and immunocompromised mice inoculated with sarcoma cells were treated with

Dox-containing water at 2 mg/ml with 10 mg/ml sucrose. *Rosa-M2rtTA/Col1a1::tetO-EWS-FLI1* mice were treated with lower concentrations of Dox (100 μg/ml to 2 mg/ml) because of early lethality. For the xenograft assay, a total of 3×10^6 *EWS-FLI1*-dependent immortalized cells, *EWS-FLI1*-dependent sarcoma cells, or ESCs/iPSCs were transplanted to immunocompromised mice. All animal experiments were approved by the CiRA Animal Experiment Committee, and the care of the animals was in accordance with institutional guidelines.

iPSC Induction and Maintenance

iPSC induction was performed by utilizing retroviral vectors (pMX-hOCT3/4, pMX-hSOX2, pMX-hKLF4, and pMX-hc-MYC; Addgene). Reprogramming factor-inducing single-cell-derived sarcoma cells were cultured in ESC media supplemented with human recombinant leukemia inhibitory factor (LIF; Wako), 2-mercaptoethanol (Invitrogen), and 50 μg/ml L-ascorbic acid (Sigma), and the established iPSCs were maintained with ESC media supplemented with LIF, 1 μM PD0325901 (Stemgent), and 3 μM CHIR99021 (Stemgent).

In Vitro Differentiation of ESC/iPSCs to Osteogenic Lineage

We employed the in vitro osteogenic differentiation protocol as described by Kim et al. (2010) with slight modifications. Briefly, 5,000 ESCs or iPSCs were cultured in a 96-well plate (Nunclon Sphere, Thermo Scientific) with ES differentiation media (Iscove's modified Dulbecco's medium, 15% FBS, penicillin/streptomycin, L-glutamine, L-ascorbic acid, transferrin, thioglycerol) for 2 days. On day 2, retinoic acid was added (final concentration, 10^{-6} M). On day 5, embryoid bodies were collected, transferred to a 6-well tissue culture dish, and cultured in osteogenic differentiation media (α minimal essential medium, 10% FBS, penicillin/streptomycin, L-glutamine, 2 nM triiodothyronine, ITS). The media were changed every other day. On day 17, RNA was extracted, and osteogenic gene expression of the induced osteogenic cells was confirmed by real-time quantitative RT-PCR. Alizarin red staining was performed on day 28.

Array Comparative Genomic Hybridization

Genomic DNA was extracted with PureLink Genomic DNA Mini Kit (Invitrogen). Array comparative genomic hybridization analysis was performed with SurePrint G3 Mouse Genome CGH Microarray Kit (Agilent) and analyzed with Agilent Genomic Workbench 7.0.

Microarray Analysis

200 ng of total RNA prepared with an RNeasy Mini Kit was subjected to cDNA synthesis with a WT Expression Kit (Ambion), and the resultant cDNA was fragmented and hybridized to a Mouse Gene 1.0 ST Array (Affymetrix). The data obtained were analyzed using GeneSpring GX software (version 13.0, Agilent Technologies).

ChIP-Seq Analysis

ChIP (formaldehyde-assisted isolation of regulatory elements) was performed as described previously (Arioka et al., 2012). Anti-HA antibody (Nacalai, HA124, 06340-54) was used for the ChIP-seq analysis. Sequencing libraries were generated using a TruSeq ChIP Sample Prep Kit (Illumina). The libraries were sequenced to generate single-end 100-bp reads using Illumina MiSeq. We used the MACS (Zhang et al., 2008) version 1.4.2 peak finding algorithm to identify regions of ChIP-seq enrichment over background with a p value 1×10^{-3}. Ngs.plot was used to analyze and visualize the mapped reads (Shen et al., 2014). The motif analysis was performed using HOMER software (Heinz et al., 2010).

Exome Analysis

Genomic DNA of SCOS#2-A1, sarcoma iPSC#2-A1, and sarcoma-iPSC#2-A1-derived secondary sarcoma was extracted with a PureLink Genomic DNA Mini Kit (Invitrogen). Whole-exome capture was done with SureSelect XT (Agilent Technologies). The exome libraries were then sequenced on a HiSeq2500 (Illumina).

ACCESSION NUMBERS

The accession number for the data reported in this article is GEO: GSE72898.

SUPPLEMENTAL INFORMATION

Supplemental Information includes Supplemental Experimental Procedures, five figures, and four tables and can be found with this article online at http://dx.doi.org/10.1016/j.stemcr.2016.02.009.

AUTHOR CONTRIBUTIONS

S.K. and Y.Y. proposed the research project, designed the experiments, performed the experiments, and wrote the manuscript. T.Y., S.K., K.S., and F.I. analyzed microarray, ChIP-seq, and exome sequencing data. A.H., K.W., T.O., H.A., and K.S. provided technical instruction. K.S., H.S., and T.Y. analyzed data.

ACKNOWLEDGMENTS

We are grateful to P. Karagiannis for critical reading of this manuscript, and T. Ukai, M. Yagi, T. Sato, and K. Osugi for technical assistance. The authors were supported in part by P-DIRECT, a Grant-in-Aid from the Ministry of Education, Culture, Sports, Science, and Technology of Japan, the Ministry of Health, Labor, and Welfare of Japan, SICORP, the Takeda Science Foundation, and the Naito Foundation.

Received: September 18, 2015
Revised: February 15, 2016
Accepted: February 16, 2016
Published: March 17, 2016

REFERENCES

Arioka, Y., Watanabe, A., Saito, K., and Yamada, Y. (2012). Activation-induced cytidine deaminase alters the subcellular localization of Tet family proteins. PLoS One *7*, e45031.

Beard, C., Hochedlinger, K., Plath, K., Wutz, A., and Jaenisch, R. (2006). Efficient method to generate single-copy transgenic mice

by site-specific integration in embryonic stem cells. Genesis *44*, 23–28.

Birsoy, K., Berry, R., Wang, T., Ceyhan, O., Tavazoie, S., Friedman, J.M., and Rodeheffer, M.S. (2011). Analysis of gene networks in white adipose tissue development reveals a role for ETS2 in adipogenesis. Development *138*, 4709–4719.

Castillero-Trejo, Y., Eliazer, S., Xiang, L., Richardson, J.A., and Ilaria, R.L., Jr. (2005). Expression of the EWS/FLI-1 oncogene in murine primary bone-derived cells results in EWS/FLI-1-dependent, Ewing sarcoma-like tumors. Cancer Res. *65*, 8698–8705.

Crompton, B.D., Stewart, C., Taylor-Weiner, A., Alexe, G., Kurek, K.C., Calicchio, M.L., Kiezun, A., Carter, S.L., Shukla, S.A., Mehta, S.S., et al. (2014). The genomic landscape of pediatric Ewing sarcoma. Cancer Discov. *4*, 1326–1341.

Dragoescu, E., Jackson-Cook, C., Domson, G., Massey, D., and Foster, W.C. (2013). Small cell osteosarcoma with Ewing sarcoma breakpoint region 1 gene rearrangement detected by interphase fluorescence in situ hybridization. Ann. Diagn. Pathol. *17*, 377–382.

Grunewald, T.G., Bernard, V., Gilardi-Hebenstreit, P., Raynal, V., Surdez, D., Aynaud, M.M., Mirabeau, O., Cidre-Aranaz, F., Tirode, F., Zaidi, S., et al. (2015). Chimeric EWSR1-FLI1 regulates the Ewing sarcoma susceptibility gene EGR2 via a GGAA microsatellite. Nat. Genet. *47*, 1073–1078.

He, B.C., Chen, L., Zuo, G.W., Zhang, W., Bi, Y., Huang, J., Wang, Y., Jiang, W., Luo, Q., Shi, Q., et al. (2010). Synergistic antitumor effect of the activated PPARgamma and retinoid receptors on human osteosarcoma. Clin. Cancer Res. *16*, 2235–2245.

Heinz, S., Benner, C., Spann, N., Bertolino, E., Lin, Y.C., Laslo, P., Cheng, J.X., Murre, C., Singh, H., and Glass, C.K. (2010). Simple combinations of lineage-determining transcription factors prime cis-regulatory elements required for macrophage and B cell identities. Mol. Cell *38*, 576–589.

Hill, D.A., O'Sullivan, M.J., Zhu, X., Vollmer, R.T., Humphrey, P.A., Dehner, L.P., and Pfeifer, J.D. (2002). Practical application of molecular genetic testing as an aid to the surgical pathologic diagnosis of sarcomas: a prospective study. Am. J. Surg. Pathol. *26*, 965–977.

Iwamoto, M., Tamamura, Y., Koyama, E., Komori, T., Takeshita, N., Williams, J.A., Nakamura, T., Enomoto-Iwamoto, M., and Pacifici, M. (2007). Transcription factor ERG and joint and articular cartilage formation during mouse limb and spine skeletogenesis. Dev. Biol. *305*, 40–51.

Kim, K., Doi, A., Wen, B., Ng, K., Zhao, R., Cahan, P., Kim, J., Aryee, M.J., Ji, H., Ehrlich, L.I., et al. (2010). Epigenetic memory in induced pluripotent stem cells. Nature *467*, 285–290.

Kinsey, M., Smith, R., and Lessnick, S.L. (2006). NR0B1 is required for the oncogenic phenotype mediated by EWS/FLI in Ewing's sarcoma. Mol. Cancer Res. *4*, 851–859.

Lee, D.F., Su, J., Kim, H.S., Chang, B., Papatsenko, D., Zhao, R., Yuan, Y., Gingold, J., Xia, W., Darr, H., et al. (2015). Modeling familial cancer with induced pluripotent stem cells. Cell *161*, 240–254.

Li, X., McGee-Lawrence, M.E., Decker, M., and Westendorf, J.J. (2010). The Ewing's sarcoma fusion protein, EWS-FLI, binds Runx2 and blocks osteoblast differentiation. J. Cell Biochem. *111*, 933–943.

Lin, P.P., Pandey, M.K., Jin, F., Xiong, S., Deavers, M., Parant, J.M., and Lozano, G. (2008). EWS-FLI1 induces developmental abnormalities and accelerates sarcoma formation in a transgenic mouse model. Cancer Res. *68*, 8968–8975.

Luo, X., Chen, J., Song, W.X., Tang, N., Luo, J., Deng, Z.L., Sharff, K.A., He, G., Bi, Y., He, B.C., et al. (2008). Osteogenic BMPs promote tumor growth of human osteosarcomas that harbor differentiation defects. Lab Invest. *88*, 1264–1277.

Merkes, C., Turkalo, T.K., Wilder, N., Park, H., Wenger, L.W., Lewin, S.J., and Azuma, M. (2015). Ewing sarcoma ewsa protein regulates chondrogenesis of Meckel's cartilage through modulation of Sox9 in zebrafish. PLoS One *10*, e0116627.

Miyagawa, Y., Okita, H., Nakaijima, H., Horiuchi, Y., Sato, B., Taguchi, T., Toyoda, M., Katagiri, Y.U., Fujimoto, J., Hata, J., et al. (2008). Inducible expression of chimeric EWS/ETS proteins confers Ewing's family tumor-like phenotypes to human mesenchymal progenitor cells. Mol. Cell Biol. *28*, 2125–2137.

Nakajima, H., Sim, F.H., Bond, J.R., and Unni, K.K. (1997). Small cell osteosarcoma of bone. Review of 72 cases. Cancer *79*, 2095–2106.

Noguera, R., Navarro, S., and Triche, T.J. (1990). Translocation (11;22) in small cell osteosarcoma. Cancer Genet. Cytogenet. *45*, 121–124.

Ohnishi, K., Semi, K., Yamamoto, T., Shimizu, M., Tanaka, A., Mitsunaga, K., Okita, K., Osafune, K., Arioka, Y., Maeda, T., et al. (2014). Premature termination of reprogramming in vivo leads to cancer development through altered epigenetic regulation. Cell *156*, 663–677.

Oshima, Y., Kawaguchi, S., Nagoya, S., Wada, T., Kokai, Y., Ikeda, T., Nogami, S., Oya, T., and Hirayama, Y. (2004). Abdominal small round cell tumor with osteoid and EWS/FLI1. Hum. Pathol. *35*, 773–775.

Postel-Vinay, S., Veron, A.S., Tirode, F., Pierron, G., Reynaud, S., Kovar, H., Oberlin, O., Lapouble, E., Ballet, S., Lucchesi, C., et al. (2012). Common variants near TARDBP and EGR2 are associated with susceptibility to Ewing sarcoma. Nat. Genet. *44*, 323–327.

Raouf, A., and Seth, A. (2000). Ets transcription factors and targets in osteogenesis. Oncogene *19*, 6455–6463.

Reya, T., Morrison, S.J., Clarke, M.F., and Weissman, I.L. (2001). Stem cells, cancer, and cancer stem cells. Nature *414*, 105–111.

Riggi, N., Cironi, L., Provero, P., Suva, M.L., Kaloulis, K., Garcia-Echeverria, C., Hoffmann, F., Trumpp, A., and Stamenkovic, I. (2005). Development of Ewing's sarcoma from primary bone marrow-derived mesenchymal progenitor cells. Cancer Res. *65*, 11459–11468.

Riggi, N., Suva, M.L., Suva, D., Cironi, L., Provero, P., Tercier, S., Joseph, J.M., Stehle, J.C., Baumer, K., Kindler, V., et al. (2008). EWS-FLI-1 expression triggers a Ewing's sarcoma initiation program in primary human mesenchymal stem cells. Cancer Res. *68*, 2176–2185.

Riggi, N., Knoechel, B., Gillespie, S.M., Rheinbay, E., Boulay, G., Suva, M.L., Rossetti, N.E., Boonseng, W.E., Oksuz, O., Cook, E.B., et al. (2014). EWS-FLI1 utilizes divergent chromatin remodeling

mechanisms to directly activate or repress enhancer elements in Ewing sarcoma. Cancer Cell *26*, 668–681.

Righi, A., Gambarotti, M., Longo, S., Benini, S., Gamberi, G., Cocchi, S., Vanel, D., Picci, P., Bertoni, F., Simoni, A., et al. (2015). Small cell osteosarcoma: clinicopathologic, immunohistochemical, and molecular analysis of 36 cases. Am. J. Surg. Pathol. *39*, 691–699.

Rossi, D.J., and Weissman, I.L. (2006). Pten, tumorigenesis, and stem cell self-renewal. Cell *125*, 229–231.

Selvanathan, S.P., Graham, G.T., Erkizan, H.V., Dirksen, U., Natarajan, T.G., Dakic, A., Yu, S., Liu, X., Paulsen, M.T., Ljungman, M.E., et al. (2015). Oncogenic fusion protein EWS-FLI1 is a network hub that regulates alternative splicing. Proc. Natl. Acad. Sci. USA *112*, E1307–E1316.

Semi, K., and Yamada, Y. (2015). iPS cell technology for dissecting the cancer epigenome. Cancer Sci. *106*, 1251–1256.

Shen, L., Shao, N., Liu, X., and Nestler, E. (2014). ngs.plot: quick mining and visualization of next-generation sequencing data by integrating genomic databases. BMC Genomics *15*, 284.

Smith, R., Owen, L.A., Trem, D.J., Wong, J.S., Whangbo, J.S., Golub, T.R., and Lessnick, S.L. (2006). Expression profiling of EWS/FLI identifies NKX2.2 as a critical target gene in Ewing's sarcoma. Cancer Cell *9*, 405–416.

Soldner, F., Hockemeyer, D., Beard, C., Gao, Q., Bell, G.W., Cook, E.G., Hargus, G., Blak, A., Cooper, O., Mitalipova, M., et al. (2009). Parkinson's disease patient-derived induced pluripotent stem cells free of viral reprogramming factors. Cell *136*, 964–977.

Takahashi, K., and Yamanaka, S. (2006). Induction of pluripotent stem cells from mouse embryonic and adult fibroblast cultures by defined factors. Cell *126*, 663–676.

Tanaka, M., Yamazaki, Y., Kanno, Y., Igarashi, K., Aisaki, K., Kanno, J., and Nakamura, T. (2014). Ewing's sarcoma precursors are highly enriched in embryonic osteochondrogenic progenitors. J. Clin. Invest. *124*, 3061–3074.

Tanaka, M., Yamaguchi, S., Yamazaki, Y., Kinoshita, H., Kuwahara, K., Nakao, K., Jay, P.Y., Noda, T., and Nakamura, T. (2015). Somatic chromosomal translocation between Ewsr1 and Fli1 loci leads to dilated cardiomyopathy in a mouse model. Sci. Rep. *5*, 7826.

Thomas, D.M., Johnson, S.A., Sims, N.A., Trivett, M.K., Slavin, J.L., Rubin, B.P., Waring, P., McArthur, G.A., Walkley, C.R., Holloway, A.J., et al. (2004). Terminal osteoblast differentiation, mediated by runx2 and p27KIP1, is disrupted in osteosarcoma. J. Cell Biol. *167*, 925–934.

Tirode, F., Laud-Duval, K., Prieur, A., Delorme, B., Charbord, P., and Delattre, O. (2007). Mesenchymal stem cell features of Ewing tumors. Cancer Cell *11*, 421–429.

Tirode, F., Surdez, D., Ma, X., Parker, M., Le Deley, M.C., Bahrami, A., Zhang, Z., Lapouble, E., Grossetete-Lalami, S., Rusch, M., et al. (2014). Genomic landscape of Ewing sarcoma defines an aggressive subtype with co-association of STAG2 and TP53 mutations. Cancer Discov. *4*, 1342–1353.

Torchia, E.C., Boyd, K., Rehg, J.E., Qu, C., and Baker, S.J. (2007). EWS/FLI-1 induces rapid onset of myeloid/erythroid leukemia in mice. Mol. Cell Biol. *27*, 7918–7934.

Yamada, K., Ohno, T., Aoki, H., Semi, K., Watanabe, A., Moritake, H., Shiozawa, S., Kunisada, T., Kobayashi, Y., Toguchida, J., et al. (2013). EWS/ATF1 expression induces sarcomas from neural crest-derived cells in mice. J. Clin. Invest. *123*, 600–610.

Yamashita, A., Morioka, M., Kishi, H., Kimura, T., Yahara, Y., Okada, M., Fujita, K., Sawai, H., Ikegawa, S., and Tsumaki, N. (2014). Statin treatment rescues FGFR3 skeletal dysplasia phenotypes. Nature *513*, 507–511.

Zhang, Y., Liu, T., Meyer, C.A., Eeckhoute, J., Johnson, D.S., Bernstein, B.E., Nusbaum, C., Myers, R.M., Brown, M., Li, W., et al. (2008). Model-based analysis of ChIP-seq (MACS). Genome Biol. *9*, R137.